Chapter 5

Hydriding / Dehydriding Studies on Low Temperature Metal Hydrides

Abstract

This chapter describes results on some low temperature alloy compositions, namely, Fe–Ti–Ni, V–Ti, and V–Ni. The Fe–Ti–Ni alloy composition shows 0.73 mass% of H_2 at a charging temperature of 103 ºC only. However, this composition releases 0.14 mass% of H_2 at discharging temperature of 150 ºC, and rest of H_2 is released at higher discharging temperature. Similarly, the V–Ti alloy composition shows 1.75 mass% of H_2 uptake at charging temperature of only 100 ºC with release of 0.46 mass% of H_2 at discharging temperature of 154 ºC. The V–Ni alloy composition indicates 1.83 mass% of H_2 at only 83 ºC charging temperature, and release of 0.88 mass% of H_2 at discharging temperature of 148 ºC. The reaction kinetics study of each system is also presented.

5.1 Introduction

In recent years, many researchers have suggested that the potential of low dehydriding temperature and high equilibrium pressure based metal hydrides need to be explored for vehicular / mobile applications. So far, most of the commercial hydrogen store alloys developed belong to AB, AB_2, A_2B, AB_5, ... etc type of chemical system. These intermetallics alloys store 1.4 wt% to 2.0 wt% of hydrogen with fast reaction kinetics and lower desorption temperature [1–5]. The resulting hydrides are also relatively more stable. This chapter deals with the hydriding / dehydriding studies on following low temperature based alloy compositions:

(i) Fe–Ti–Ni alloy composition
(ii) V–Ti alloy composition
(iii) V–Ni alloy composition

Properties and preparation of alloy compositions have been discussed in chapter 3. The lower desorption temperature based alloy compositions using a combination of metal alloying (Fe, Ti, V and Ni) have been synthesized by high energy planetary ball milling for hydrogen storage application. Detailed characterization and kinetics studies on low temperature Fe–Ti–Ni, V–Ti and V–Ni alloy compositions are presented in this chapter.

5.2 Fe–Ti–Ni Alloy Composition

5.2.1 Sample Preparation

Fe–Ti–Ni system is synthesized using Fe, Ti and Ni powders with a minimum of 99% purity. The milling experiments are conducted in a planetary ball mill. The detailed technical parameters of ball mill are presented in chapter 3. The chemical composition of Fe–Ti–Ni system is prepared with 47.5 at% of Iron, 47.5 at% of Titanium and 5.0 at% of Nickel. The weight calculation of individual elements of this composition is given as under:

The atomic fraction of each element in the $Fe_{47.5\%}Ti_{47.5\%}Ni_{5\%}$ composition is computed as below:

$$Fe^{af} = \frac{Fe^{w} / Fe^{aw}}{Fe^{w} / Fe^{aw} + Ti^{w} / Ti^{aw} + Ni^{w} / Ni^{aw}} \quad \text{---------- (5.1)}$$

$$Ti^{af} = \frac{Ti^{w} / Ti^{aw}}{Fe^{w} / Fe^{aw} + Ti^{w} / Ti^{aw} + Ni^{w} / Ni^{aw}} \quad \text{---------- (5.2)}$$

$$Ni^{af} = \frac{Ni^{w} / Ni^{aw}}{Fe^{w} / Fe^{aw} + Ti^{w} / Ti^{aw} + Ni^{w} / Ni^{aw}} \quad \text{---------- (5.3)}$$

Where, Fe^{af}, Ti^{af} and Ni^{af} are the atomic fraction of Fe, Ti and Ni, respectively; Fe^{w}, Ti^{w} and Ni^{w} are the weight of Fe, Ti and Ni, respectively; and Fe^{aw}, Ti^{aw} and Ni^{aw} are the atomic weight of Fe, Ti and Ni, respectively.

Next, using Eqns. 5.1 to 5.3, weight of each element in the $Fe_{47.5\%}Ti_{47.5\%}Ni_{5\%}$ composition can be computed as:

$$Fe^{w} = \frac{Fe^{aw} \times Fe^{af}}{Fe^{af} + Ti^{af} + Ni^{af}} = 26.53 \quad \text{---------- (5.4)}$$

$$Ti^{w} = \frac{Ti^{aw} \times Ti^{af}}{Fe^{af} + Ti^{af} + Ni^{af}} = 22.75 \quad \text{---------- (5.5)}$$

$$Ni^{w} = \frac{Ni^{aw} \times Ni^{af}}{Fe^{af} + Ti^{af} + Ni^{af}} = 2.94 \quad \text{---------- (5.6)}$$

Therefore, for 20 gm composition, the weight of Fe is computed as 10.16 gm, the weight of Ti is 8.71 gm and Ni is 1.13 gm for $Fe_{47.5\%}Ti_{47.5\%}Ni_{5\%}$ composition.

5.2.2 Characterization Study

Micrographs showing the morphology of the pure Fe and Ti without milling and the synthesized Fe–Ti–Ni composition after 40 h milled are shown in Fig. 5.1. The mean particle size of Iron particles is measured as 56.6 ± 22 μm and Titanium particles is 141 ± 60.8 μm (without milled) by lineal analysis of SEM micrographs. The mean

particle size of the synthesized Fe–Ti–Ni composition particles is obtained as 8.37 ± 5.7 μm.

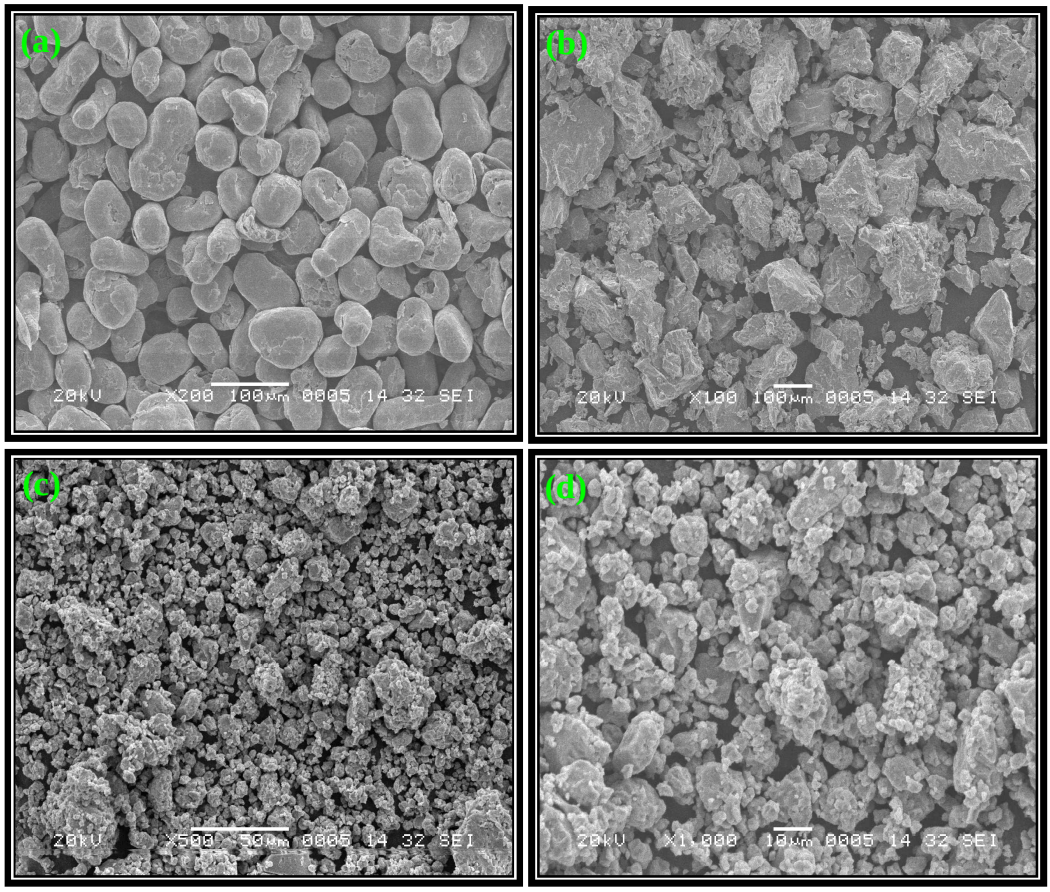

Fig. 5.1: SEM micrographs of (a) Pure Fe without milled, (b) Pure Ti without milled; and Fe–Ti–Ni composition (40 h milled) (c) 500 X and (d) 1000 X

EDS analysis is conducted in SEI (secondary electron image) mode at accelerating voltage of 20 kV and 100 X magnification on the synthesized alloy. Results indicate that the synthesized alloy has 48.96 wt% Iron, 44.56 wt% Titanium, 3.56 wt% Nickel and 2.92 wt% Chromium, which match closely with targeted compositions (47.5 at% for Mg, 47.5 at% for Fe and 5 at% for Ni). Chromium peak appears due to its presence as an impurity. A typical EDS spectrum of the synthesized alloy composition is shown in Fig. 5.2.

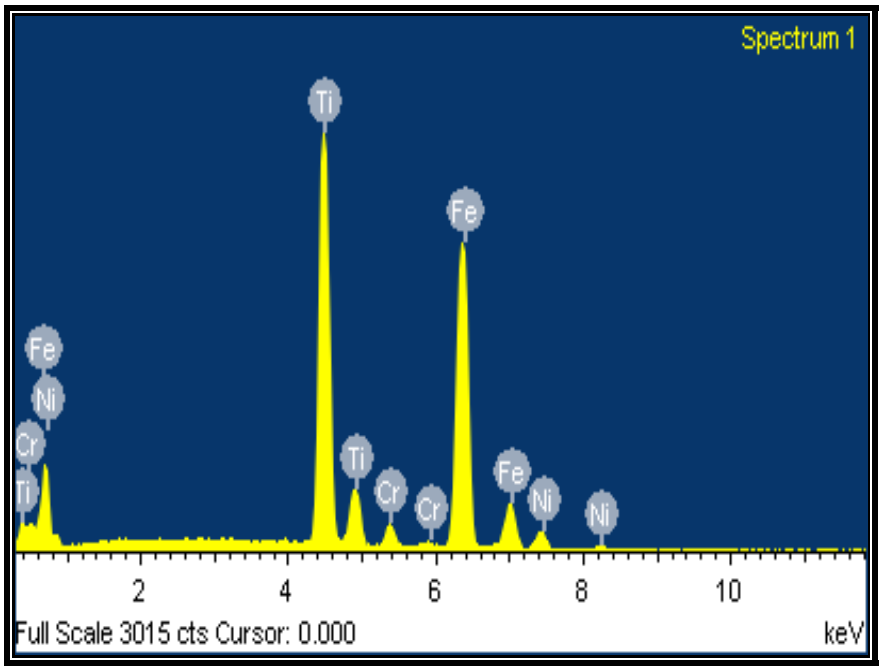

Fig. 5.2: EDS spectra of Fe–Ti–Ni alloy composition

The XRD spectrum of the Fe–Ti–Ni alloy composition showing a plot of intensity in arbitrary units as a function of diffraction angle, 2θ, is presented in Fig. 5.3. Predominant peaks corresponding to Fe, Ti and Ni, along with the peaks corresponding to the phases, $Fe+2TiO_3$ and FeO are seen.

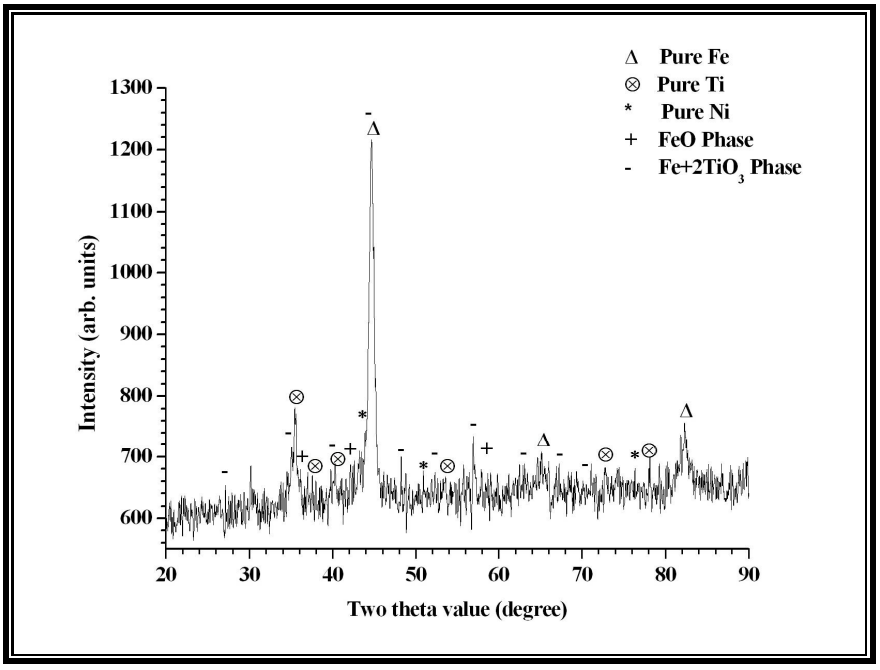

Fig. 5.3: XRD spectra of the synthesized Fe–Ti–Ni alloy composition

The diffraction peaks could be accurately indexed and correlated with Fe phase, Ti phase, Ni phase, Fe+2TiO_3 phase and FeO phase. The Bravais lattice system of these phases being cubic (cell parameters, a: 2.8607 Å), hexagonal (cell parameter, a: 2.9200 Å & c: 4.6700 Å), cubic (cell parameter, a: 3.5400 Å), rhombic (cell parameter, a: 5.0800 Å & c: 14.0300 Å) and cubic (cell parameter, a: 4.2900 Å), respectively. Further, the mean crystallite/grain size of these phases is measured as 21.91 nm, 10.04 nm, 37.29 nm, 11.53 nm and 21.41 nm, respectively.

5.2.3 Hydriding / Dehydriding Analysis

In Fig. 5.4 (a) and (b), the charging and discharging kinetics are presented, respectively, of the synthesized Fe–Ti–Ni composition. Specifically, Fig. 5.4(a) presents the kinetics plots of the hydriding reaction at 100 ℃ temperature and an initial hydrogen charging pressure of 30 bar. Hydrogen up-take capacity of this composition is rapid initially and after then, it decreases with time. The maximum hydrogen storage capacity is measured as 0.73 mass% at 100 ºC charging temperature. Note that as the hydriding reaction time is nearly 80 to 90 minutes.

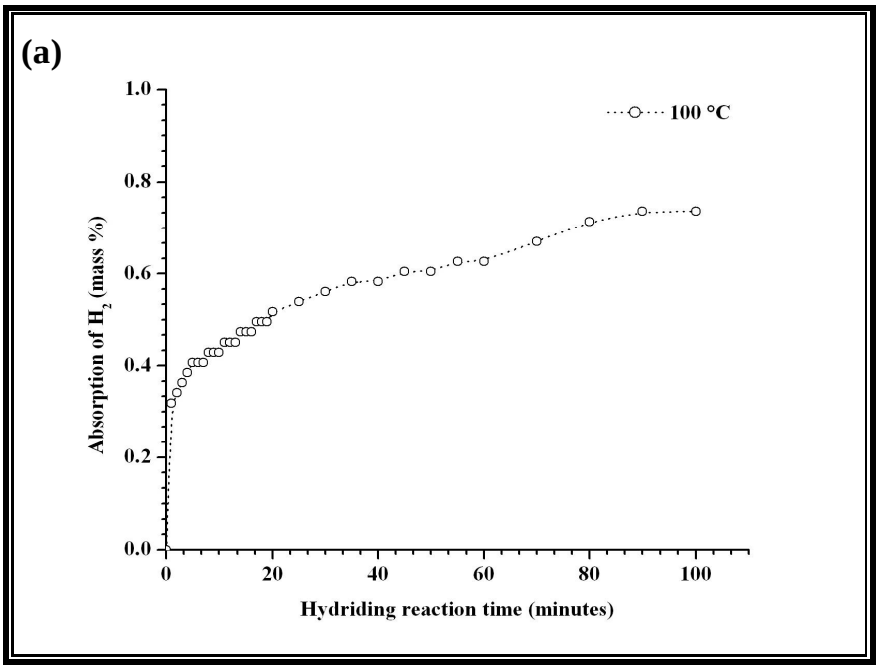

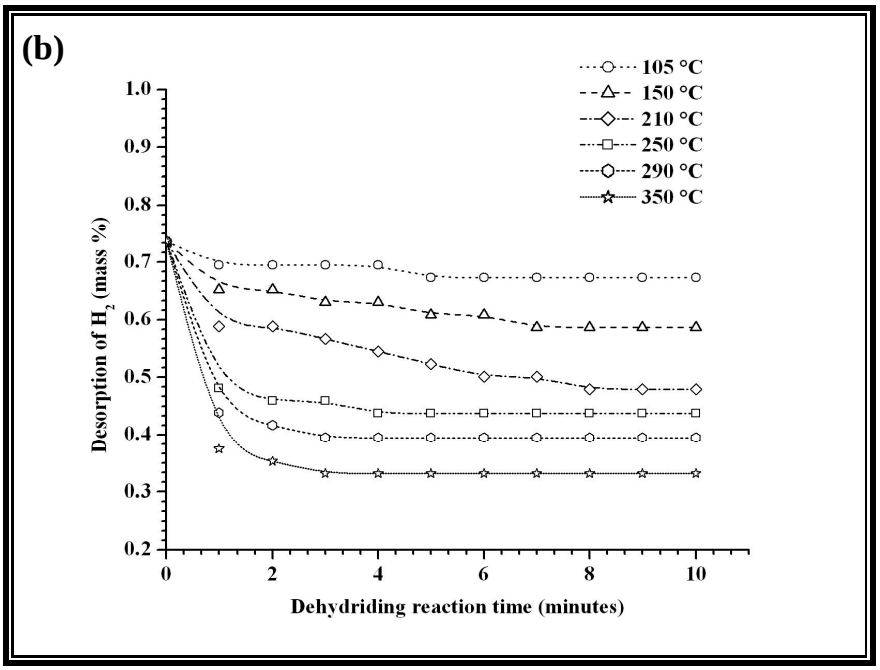

Fig. 5.4: Kinetics curve of Fe–Ti–Ni composition: (a) Charging kinetics and (b) Discharging kinetics

In Fig. 5.4(b), dehydriding of hydrogen at different temperatures is presented, which shows that increase of temperature results in a monotonic increase of hydrogen released along with the dehydriding rate. This shows that 55 % of hydrogen is desorbed first 5 minutes for the synthesized Fe–Ti–Ni composition at 350 ºC. Mass % of hydrogen released from this hydrided composition is measured as 0.06 %, 0.14 %, 0.26 %, 0.30 %, 0.34 % and 0.40 % at 105 ºC, 150 ºC, 210 ºC, 250 ºC, 290 ºC and 350 ºC, respectively.

5.3 V–Ti Alloy Composition

5.3.1 Sample Preparation

The ternary V–Ti system is synthesized using V and Ti powders with a minimum of 99% purity. The milling experiments are conducted in a planetary ball mill. The detailed technical parameters of ball mill are presented in chapter 3. The chemical composition of V–Ti composition is prepared with 66.67 at% of Vanadium and 33.33 at% of Titanium. The weight calculation of elements of this composition is given as under:

The atomic fraction of each element in the $V_{66.67\%}Ti_{33.33\%}$ composition is given as:

$$V^{af} = \frac{V^{w} / V^{aw}}{V^{w} / V^{aw} + Ti^{w} / Ti^{aw}} \qquad \text{---------- (5.7)}$$

$$Ti^{af} = \frac{Ti^{w} / Ti^{aw}}{V^{w} / V^{aw} + Ti^{w} / Ti^{aw}} \qquad \text{---------- (5.8)}$$

Where, V^{af} and Ti^{af} are the atomic fraction of V and Ti, respectively; V^{w} and Ti^{w} are the weight of V and Ti, respectively; and V^{aw} and Ti^{aw} are the atomic weight of V and Ti, respectively.

Next, using Eqns. 5.1 to 5.3, weight of each element in the $V_{66.67\%}Ti_{33.33\%}$ composition is computed as:

$$V^{w} = \frac{V^{aw} \times V^{af}}{V^{af} + Ti^{af}} = 33.96 \qquad \text{---------- (5.9)}$$

$$Ti^{w} = \frac{Ti^{aw} \times Ti^{af}}{V^{af} + Ti^{af}} = 15.96 \qquad \text{---------- (5.10)}$$

Therefore, for 20 gm composition, the weight of V is computed as 13.61 gm and Ti is 6.39 gm for $V_{66.67\%}Ti_{33.33\%}$ composition.

5.3.2 Characterization Study

Micrograph showing the morphology of the synthesized V–Ti composition after 40 h milling is shown in Fig. 5.5 at different magnifications. The mean particle size of the synthesized V–Ti composition particles is obtained as 6.24 ± 2. 6 μm by lineal analysis of SEM micrographs. EDS analysis is conducted in SEI (secondary electron image) mode at accelerating voltage of 15 kV and 80 X magnification on the synthesized alloy. Results indicate the synthesized alloy has 65.25 wt% Vanadium, 33.86 wt% Titanium and 0.89 wt% Nickel, which closely match with targeted

compositions (66.67 at% for V and 33.33 at% for Ti). Nickel peak is seen due to its presence as an impurity. A typical EDS spectrum of the synthesized alloy composition is shown in Fig. 5.6.

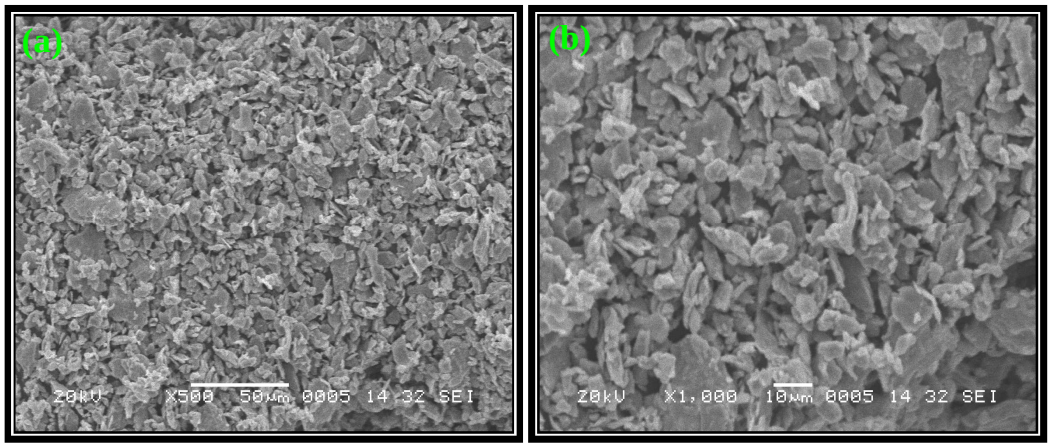

Fig. 5.5: SEM micrograph of V–Ti composition (40 h milled): (a) 500 X and (b) 1000 X

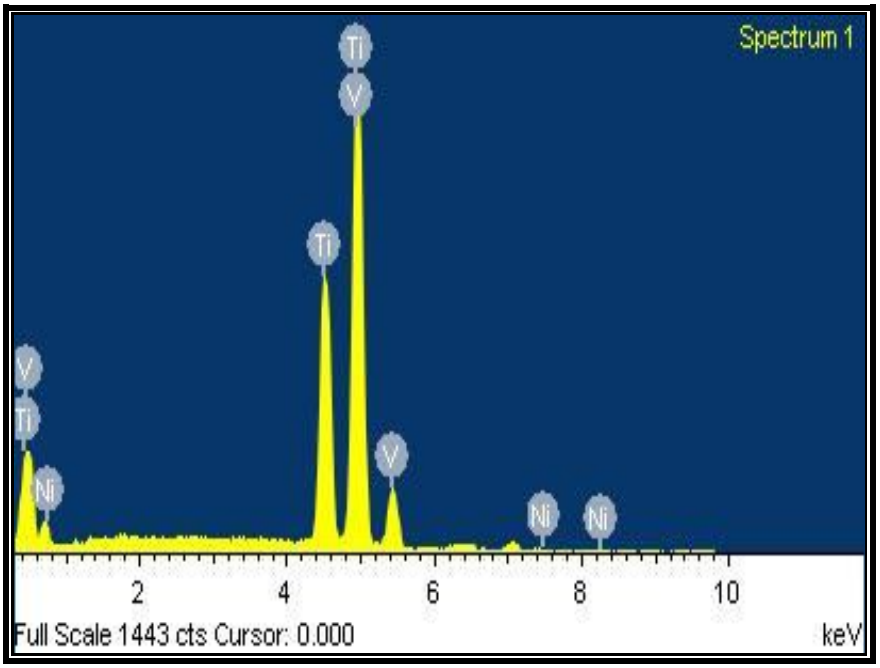

Fig. 5.6: EDS spectra of V–Ti alloy composition

The XRD spectrum of the synthesized alloy is presented in Fig. 5.7. Predominant peaks corresponding to V, Ti, Ni and TiV are seen. The various diffraction peaks could be accurately indexed and correlated with V phase (Bravais

lattice: cubic, a: 3.0400 Å), Ti phase (Bravais lattice: hexagonal, a: 2.9200 Å & c: 4.6700 Å), Ni phase (Bravais lattice: cubic, a: 3.5175 Å) and TiV phase (Bravais lattice: cubic, a: 3.1650 Å). Further, the mean crystallite/grain size of these phases is measured as 8.15 nm, 10.04 nm, 9.55 nm and 10.04 nm, respectively.

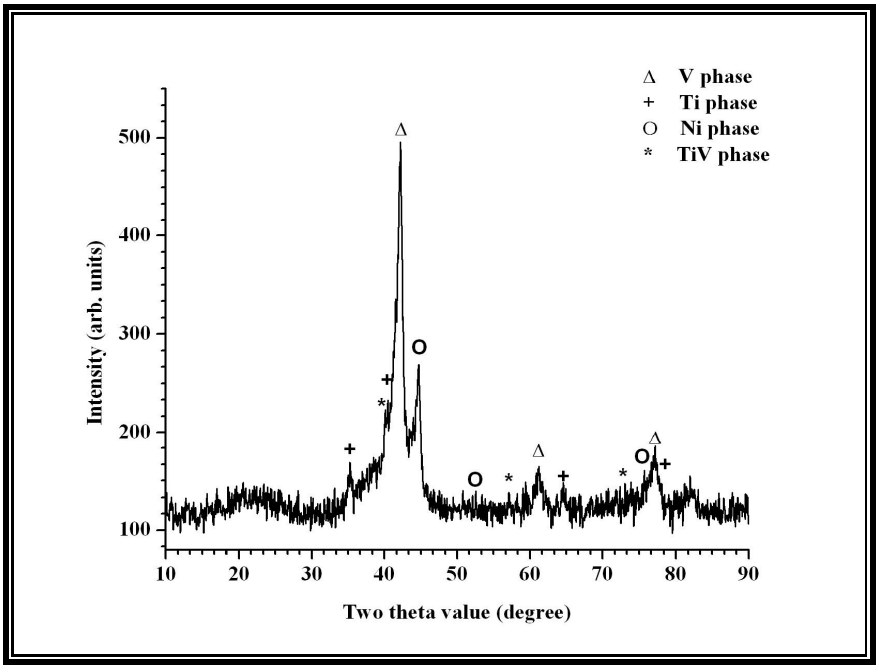

Fig. 5.7: XRD spectra of the synthesized V–Ti alloy composition

5.3.3 Hydriding / Dehydriding Analysis

In Fig. 5.8 (a) and (b), the charging and discharging kinetics are presented, respectively, of the synthesized V–Ti composition. Specifically, Fig. 5.8(a) presents the kinetics plots of the hydriding reaction at 100 ℃ temperature and an initial hydrogen charging pressure of 30.76 bar. Hydrogen up-take capacity of this composition is rapid initially and after then, it decreases with time. The maximum hydrogen storage capacity is measured as 1.75 mass% at 100 ºC charging temperature. Note that as the maximum hydriding reaction time is occurred within first 30 minutes.

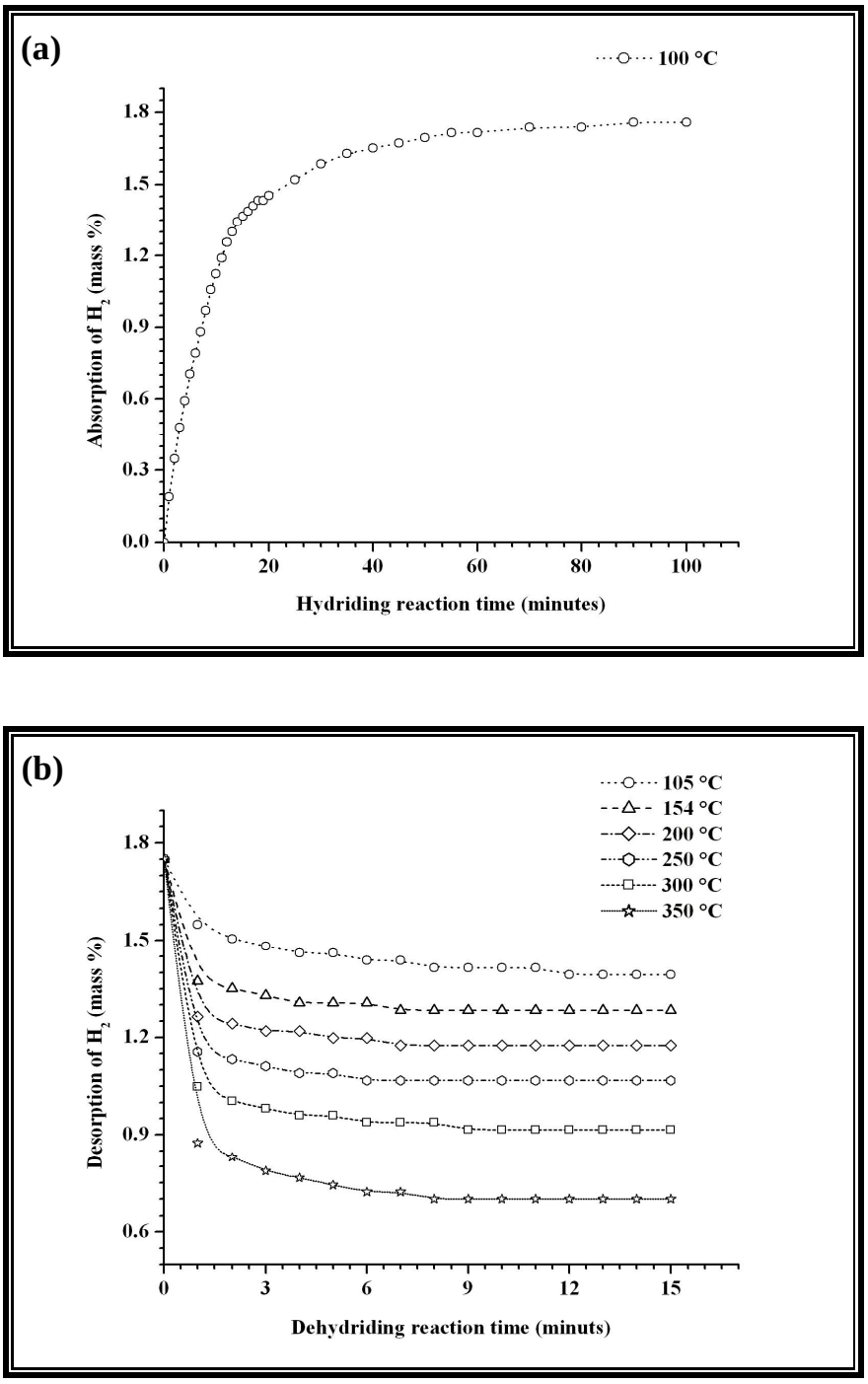

Fig. 5.8: Kinetics curve of V–Ti composition: (a) Charging kinetics and (b) Discharging kinetics

In Fig. 5.8(b), dehydriding of hydrogen at different temperatures is presented, which shows that the increase of temperature results in a monotonic increase of hydrogen released along with the dehydriding rate. This shows that greater than 90 %

of hydrogen is desorbed within 5 minutes for the synthesized V–Ti composition at 350 ºC. Mass % of hydrogen released from this hydrided composition is measured as 0.36 %, 0.46 %, 0.57 %, 0.68 %, 0.83 % and 1.05 % at 105 ºC, 154 ºC, 200 ºC, 250 ºC, 300 ºC and 350 ºC, respectively.

5.4 V–Ni Alloy Composition

5.4.1 Sample Preparation

V–Ni system is synthesized using V and Ni powders with a minimum of 99% purity. The milling experiments are conducted in a planetary ball mill. The detailed technical parameters of ball mill are presented in chapter 3. The chemical composition of V–Ni system is prepared with 95 at% of Vanadium and 5.0 at% of Nickel. The weight calculation of elements of this composition is given as under:

The atomic fraction of each element in the $V_{95\%}Ni_{5\%}$ composition is given as:

$$V^{af} = \frac{V^{w} / V^{aw}}{V^{w} / V^{aw} + Ni^{w} / Ni^{aw}} \qquad \text{---------- (5.11)}$$

$$Ni^{af} = \frac{Ni^{w} / Ni^{aw}}{V^{w} / V^{aw} + Ni^{w} / Ni^{aw}} \qquad \text{---------- (5.12)}$$

Where, V^{af} and Ni^{af} are the atomic fraction of V and Ni, respectively; V^{w} and Ni^{w} are the weight of V and Ni, respectively; and V^{aw} and Ni^{aw} are the atomic weight of V and Ni, respectively.

Next, using Eqns. 5.11 and 5.12, weight of each element in the $V_{95\%}Ni_{5\%}$ composition is computed as:

$$V^{w} = \frac{V^{aw} \times V^{af}}{V^{af} + Ni^{af}} = 48.39 \qquad \text{---------- (5.13)}$$

$$Ni^{w} = \frac{Ni^{aw} \times Ni^{af}}{V^{af} + Ni^{af}} = 2.94 \qquad \text{---------- (5.14)}$$

Therefore, for 20 gm composition, the weight of V is computed as 18.85 gm and Ni is 1.15 gm for $V_{95\%}Ni_{5\%}$ composition.

5.4.2 Characterization Study

Micrographs showing the morphology of the synthesized V–Ni alloy (after 15 h milling) are shown in Fig. 5.9 at different magnifications. For the synthesized V–Ni alloy, the particle size is measured as 12.5 ± 2.9 μm using lineal analysis of SEM micrographs.

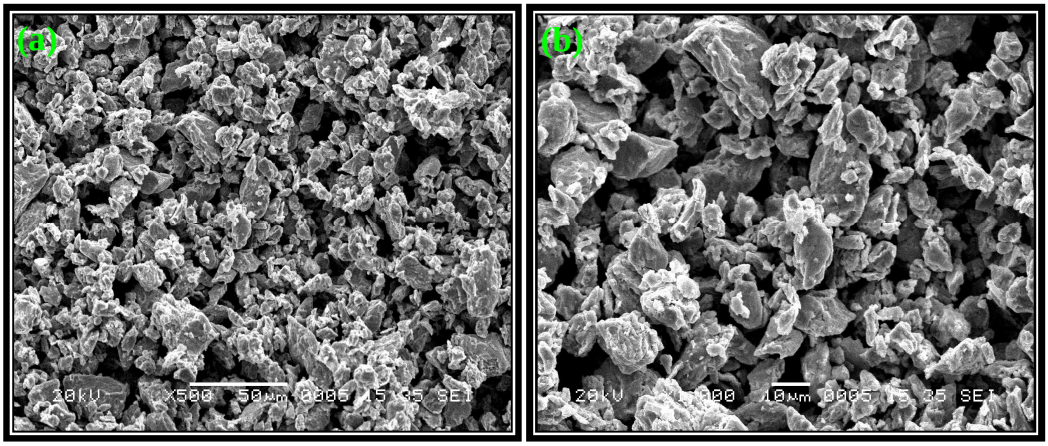

Fig. 5.9: SEM micrographs of V–Ni alloy after 15 h milling: (a) 500 X and (b) 1000 X

EDS analysis is conducted in SEI (Secondary Electron Image) mode at an accelerating voltage of 20 kV and 100 X magnification on the synthesized alloy. Results (presented in Table–5.1) indicate that the measured elemental composition matches closely with the targeted composition. Typical EDS spectra of the synthesized composition is shown in Fig. 5.10.

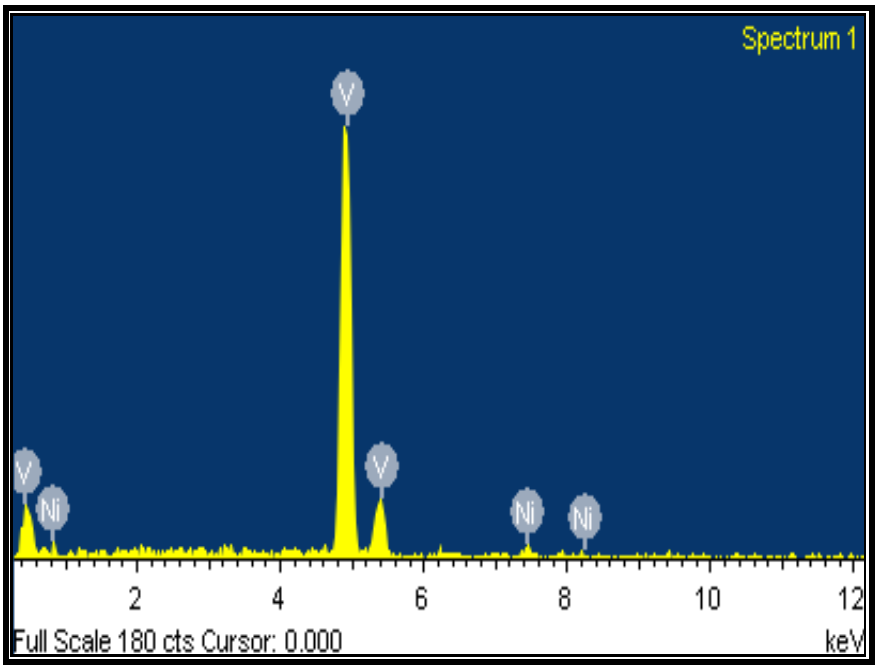

Fig. 5.10: EDS spectra of synthesized V–Ni alloy composition

Table–5.1: Elemental composition of the synthesized V–Ni alloy composition

Sr. No.	Elements	Target		Obtain	
		Weight %	Atomic %	Weight %	Atomic %
1	V	94.28	95	94.03	94.78
2	Ni	5.72	5	5.97	5.22

The XRD spectrum of the synthesized alloy is presented in Fig. 5.11. Predominant peaks corresponding to V, Ni, NiV_3, Ni_2V, and Ni_2V_3 are seen. The various diffraction peaks could be accurately indexed and correlated with V phase (Bravais lattice: cubic, a: 3.0400 Å), Ni phase (Bravais lattice: cubic, a: 3.5176 Å), NiV_3 phase (Bravais lattice: cubic, a: 4.7115 Å), Ni_2V phase (Bravais lattice: orthorhombic, a: 2.5590 Å, b: 7.6410 Å & c: 3.5490 Å), and NiV_3 phase (Bravais lattice: tetragonal, a: 8.9660 Å & c: 4.6410 Å). Further, the mean crystallite/grain size of these phases was measured as 8.33 nm, 9.16 nm, 9.4 nm, 8.92 nm, and 8.34 nm, respectively.

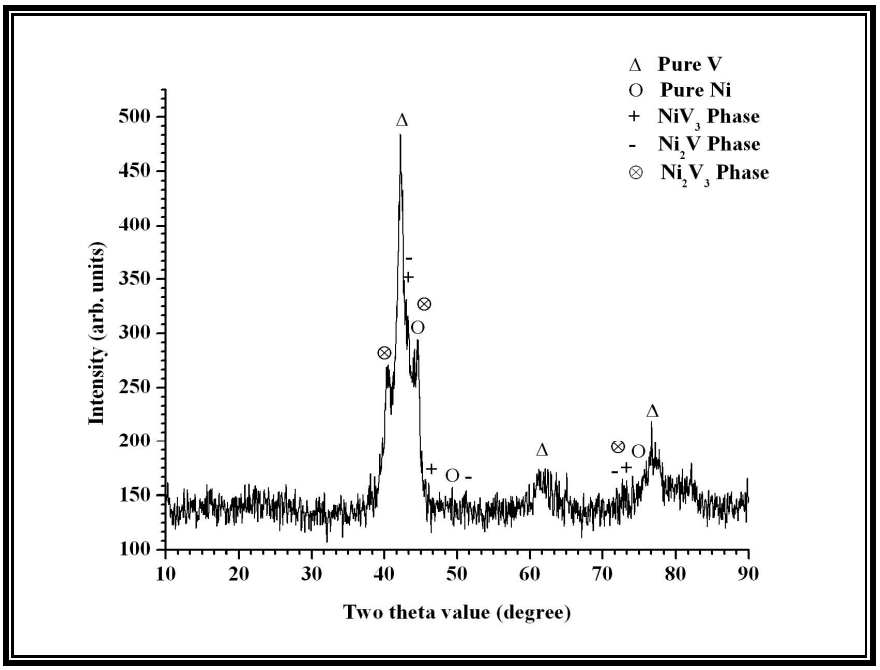

Fig. 5.11: XRD spectra of the synthesized V–Ni alloy composition

5.4.3 Hydriding/dehydriding Analysis

In Fig. 5.12 (a) and (b), the charging and discharging kinetics are presented, respectively, of the synthesized V–Ni composition.

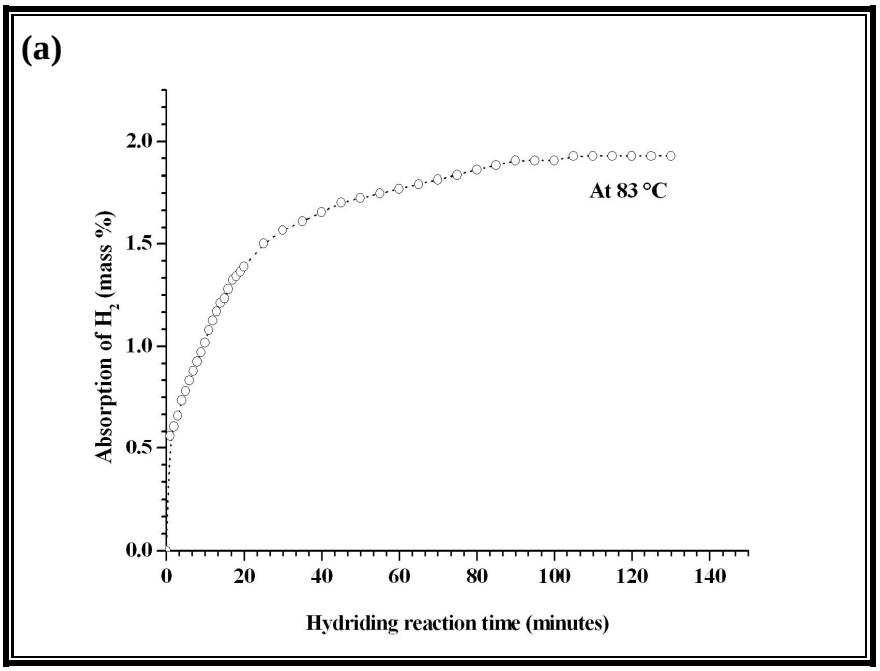

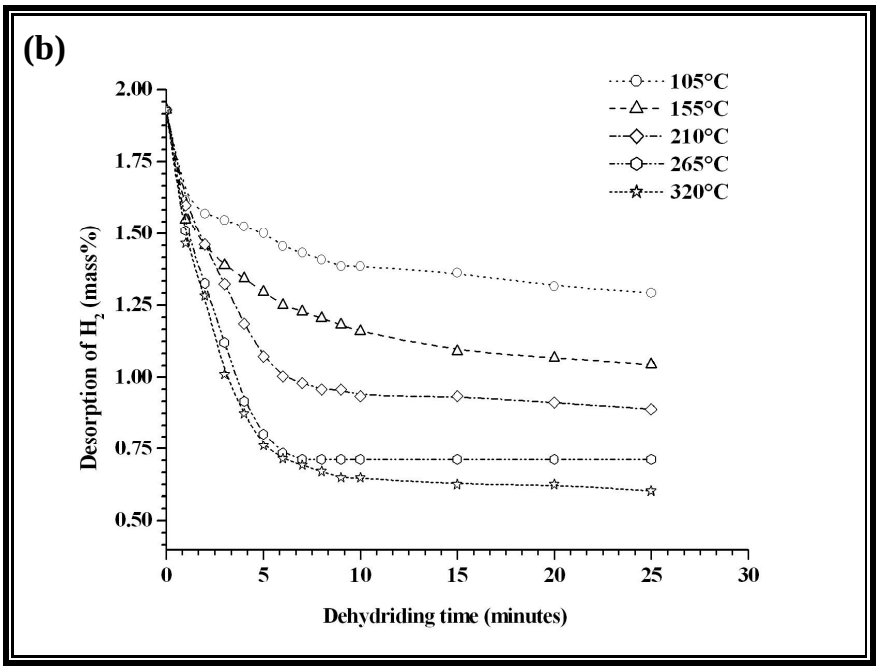

Fig. 5.12: Kinetics curve of V–Ni composition: (a) Charging kinetics and (b) Discharging kinetics

Specifically, Fig. 5.12(a) presents the kinetics plots of the hydriding reaction at 83 °C temperature and an initial hydrogen charging pressure of 30.14 bar. Hydrogen up-take capacity of this composition is rapid initially and thereafter, it decreases with time. The maximum hydrogen storage capacity is measured as 1.92 mass% at 83 ºC charging temperature [6]. Note that as the hydriding reaction time for steady state occurs within 60 minutes.

In Fig. 5.12(b), dehydriding of hydrogen at different temperatures is presented, which shows that increase of temperature results in a monotonic increase of hydrogen released along with the dehydriding rate. This shows that greater than 90 % of hydrogen is desorbed within 5 minutes for the synthesized V–Ni composition at 320 ºC. Mass % of hydrogen released from this hydrided composition is measured as 0.66 %, 0.88 %, 1.04 %, 1.22 % and 1.33 % at 105 ºC, 155 ºC, 210 °C, 265 ºC and 320 ºC, respectively.

REFERENCES

1. G. Sandrock, State–of–the art review of Hydrogen storage in reversible metal hydrides for military fuel cell applications, *Department of the Navy, SunTech Inc., Final Report*, 24 July (1997) 25 – 97.
2. C. Y. Seo, J. H. Kim, P. S. Lee and J. Y. Lee, *J. of Alloys and Compounds*, **348** (2003) 252–257.
3. M. Latroche, *J. of Physics and Chemistry of Solids,* **65** (2004) 517–522.
4. X. B. Yu, S. L. Feng, Z. Wu, B. J. Xia, N. X. Xu, *J. of Alloys and Compounds*, **393** (2005) 129–134.
5. A. Kinaci and M. K. Aydinol, *Int. J. of Hydrogen Energy,* **32** (2007) 2466 – 2474.
6. K. G. Bambhaniya, G. S. Grewal, V. Shrinet, N. L. Singh and T. P. Govindan, Synthesis of a V–Ni Alloy with Low Temperature Hydriding Characteristics for Hydrogen Energy Storage, *Int. J. of Green Energy* (communicated).